MASTER

CONF--751125--30

PREPRINT UCRL-77263

Lawrence Livermore Laboratory

ANALYSIS OF THE STEADY-STATE OPERATION OF
VACUUM SYSTEMS FOR FUSION MACHINES

T. R. Roose
M. A. Hoffman
G. A. Carlson

November 3, 1975

This paper was prepared for submittal to the Proceedings of the Sixth Symposium on Engineering Problems of Fusion Research, San Diego, California, November 18 through 21, 1975.

ANALYSIS OF THE STEADY-STATE OPERATION OF VACUUM SYSTEMS FOR FUSION MACHINES*

T. R. Roose

M. A. Hoffman

G. A. Carlson

Lawrence Livermore Laboratory, University of California
Livermore, California 94550

Summary

We have written a computer code named GASBAL to calculate the steady-state vacuum system performance of multi-chamber mirror machines as well as rather complex conventional multi-chamber vacuum systems. Application of the code, with some modifications, to the quasi-steady tokamak operating period should also be possible. Basically, GASBAL analyzes free molecular gas flow in a system consisting of a central chamber (the plasma chamber) connected by conductances to an arbitrary number of one- or two-chamber peripheral tanks. Each of the peripheral tanks may have vacuum pumping capability (pumping speed), sources of cold gas, and sources of energetic atoms. The central chamber may have actual vacuum pumping capability, as well as a plasma capable of ionizing injected atoms and impinging gas molecules and "pumping" them to a peripheral chamber. We successfully applied the GASBAL code to the preliminary design of a large mirror machine experiment — LLL's MX.

Introduction

A magnetically confined thermonuclear plasma can exist only in a high vacuum. Possible sources of cold background gas in a fusion machine include gas leaks, gas flow from neutral beam injectors, and gas reflux from surfaces bombarded by energetic ions and atoms. The designers of fusion experiments and fusion reactors must provide for the effective pumping of this cold gas

We have written a computer code named GASBAL to analyze the steady-state operation of vacuum systems for fusion machines. While the original intent of the analysis was to provide design information for LLL's MX experiment, the code was written in a general manner so as to be applicable to the vacuum analysis of many fusion machines and components.

Physical Model

To illustrate the physical model, we describe the vacuum system proposed for MX. From a vacuum system viewpoint, the primary components of MX are two neutral beam injector tanks, two dump tanks, and a main tank (Fig. 1). The main tank is further divided into the plasma chamber (the volume within the magnet coils), two mirror leakage tanks (also referred to as end tanks), and a side tank. The injector tanks provide pumping for the large amount of cold gas introduced by the ion sources of the neutral beam injectors. The dump tanks provide pumping for the neutral beam particles that penetrate through the plasma. The end tanks pump the mirror leakage particles, and the side tank provides an additional sink for random gas in the plasma chamber.

Each of the seven peripheral tanks is connected to the plasma chamber by an orifice or duct. The injector and dump tanks are double-chambered with connecting ducts. Cryopanel gas pumping surfaces line the chamber walls of all seven peripheral tanks.

A typical two-chamber tank system along with the notation for the cold gas conductances, C, and the pumping speeds, S, is shown in Fig. 2. Provision is made in our analysis for tapered ducts with cryopanel pumping surfaces inside the ducts by allowing the assignment of different C's and S's for flows in opposite directions through the ducts.

The steady-state cold gas equations for the representative two-chamber tank system K of Fig. 2 are as follows:

tank K1 equation

$$P_1(K)\left[S_1(K) + S_{C11}(K) + C_{11}(K)\right] - P_2(K)C_{12}(K) = Q_{1S}(K); \qquad (1)$$

tank K2 equation

$$-P_1(K)C_{11}(K) + P_2(K)\left[S_2(K) + S_{C22}(K) + S_{C12}(K) + C_{22}(K) + C_{12}(K)\right] - P_{PC}\,C_{2P}(K) = Q_{2S}(K)\ . \qquad (2)$$

The total of all the various cold gas source flows into tanks K1 and K2 are $Q_{1S}(K)$ and $Q_{2S}(K)$, respectively.

The above set of 2N equations for N two-chamber systems contains 2N + 1 unknown pressures: the N different $P_1(K)$ values, the N different $P_2(K)$ values and the plasma chamber cold gas pressure, P_{PC}. The additional equation for a complete specification of the problem is the steady-state equation for the cold background gas flows into and out of the plasma chamber:

*Work performed under the auspices of the United States Energy Research and Development Administration, under contract No. W-7405-Eng-48.

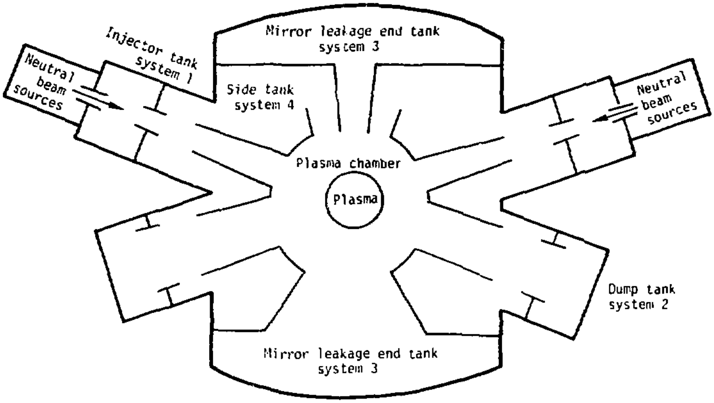

Fig. 1. Schematic diagram of the MX experimental mirror machine illustrating the multichamber vacuum system.

$$Q_{CWS} + Q_{CN(TOT)} = Q_{CP} + Q_{CD(TOT)} . \qquad (3)$$

This will be referred to as the plasma chamber equation. The left-hand-side represents the two types of cold gas flows into the plasma chamber:

Q_{CWS} = Net source of cold gas that is refluxed off the plasma chamber wall

$Q_{CN(TOT)}$ = sum of the net flows of cold gas from each of the N tank systems into the plasma chamber

$$= \sum_{K=1}^{N} Q_{CN}(K)$$

$$= \sum_{K=1}^{N} \left\{P_2(K)C_{22}(K) - P_{PC}\left[C_{2P}(K) + S_{C2P}(K)\right] + Q_D(K)\right\} .$$

The first two terms in $Q_{CN}(K)$ represent the pressure-dependent flows of cold gas into and out of the plasma chamber, while the last term, $Q_D(K)$, represents the directed or free-streaming component of $Q_{1S}(K)$ and/or $Q_{2S}(K)$ which flows directly from a neutral beam source into the plasma chamber.

The right-hand-side of Eq. (3) represents the flow of cold gas from the plasma chamber as a result of the "pumping" action of the plasma, ie., the ionization of cold gas atoms by the plasma and the immediate loss of the cold ions out of the mirrors:

Q_{CP} = the randomized cold background gas that impinges on the plasma.

$$= P_{PC}S_{PL}$$

$Q_{CD(TOT)}$ = sum of the portions of the cold gas flow from each tank system that impinge directly on the plasma before they can be randomized in the plasma chamber

$$= \sum_{K=1}^{N} Q_{CD}(K)$$

$$= \sum_{K=1}^{N} \left[F_{CD}(K)P_2(K)C_{22}(K) + Q_D(K)\right] ,$$

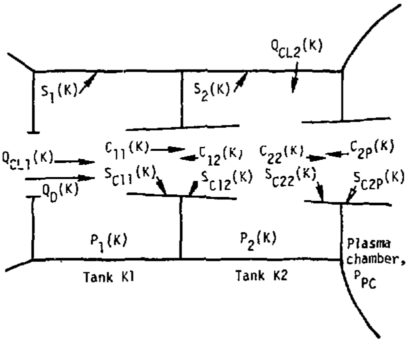

Fig. 2. Typical two-chamber tank system K showing the notation used; the general case of tapered ducts with internal cryopanels is assumed.

where $F_{CD}(K)$ is the fraction of random gas flowing from tank K2 into the plasma chamber that impinges directly onto the plasma.

The set of 2N + 1 equations in the 2N + 1 unknown pressures can be solved once we know the effective cold gas source terms $Q_{1S}(K)$, $Q_{2S}(K)$ and Q_{CWS}. The major contribution to $Q_{1S}(K)$ in the injector tanks will usually be the cold gas leakage from the neutral beam sources; this is normally a known or specified input parameter. If Q_{CWS}, $Q_{2S}(K)$, and the other contributions to $Q_{1S}(K)$ were known constants or simple functions of known input parameters, the solution to the problem would be relatively straightforward. Unfortunately, some terms in $Q_{1S}(K)$, $Q_{2S}(K)$, and Q_{CWS} are strongly coupled to the hot particle flows and, consequently, are rather complicated to evaluate in the general case.

To illustrate these complications, a simplified flow diagram of the principal hot and cold particle flows in a typical mirror fusion machine is given in Fig. 3. Hot particle flows are represented by dashed lines and cold particle flows by solid lines. Entering the plasma chamber from the injector tanks is the portion of the neutral beam flow that reaches the plasma chamber and impinges on the plasma, Q_{HP}, as well as the net cold gas outflow Q_{CN}. The part of Q_{CN} that randomizes, Q_{CR}, becomes part of the random cold background gas that produces the plasma chamber background pressure, P_{PC}. In steady-state, some of this gas is pumped out by the plasma and some leaks out of the plasma chamber into each of the N peripheral tank systems (only the leakage into the dump tanks is shown in Fig. 3). The remainder of Q_{CN}, referred to as Q_{CD} above, is the portion that impinges directly on the plasma. All of the cold gas particles that impinge on the plasma are assumed to ionize and to flow to the end tanks as indicated by Q_{CM} on Fig. 3.

In the process of pumping these cold gas flows, a certain fraction of the encounters with the hot plasma ions results in undesirable charge exchange reactions. Some of the hot neutrals produced by the charge exchange will impinge on the plasma chamber walls, thereby contributing to the total hot particle flow to the wall, Q_{HW}. The remainder of these hot neutrals, Q_{HZ}, enter the N peripheral tank systems (only the flow into the dump tanks is shown on Fig. 3). These hot neutral particles are assumed to impinge on the walls of the peripheral tanks where they are converted to cold neutral molecules. Consequently, the hot charge-exchange neutrals become a contribution to the sources of cold gas in the peripheral tanks (Q_{1S} and Q_{2S}). This contribution is, in part, a function of the pressure $P_2(K)$ in injector tank 2 through the charge exchange caused by Q_{CD}. We see that this chain of events leads to a coupling between the peripheral tank pressures and flows, which complicates the evaluation of the source terms in Eqs. (1) and (2).

The injected neutral beam flow, Q_{HP}, can also contribute directly and indirectly to the sources of cold gas Q_{1S} and Q_{2S} in every tank system. For the simplified case shown in Fig. 3, the untrapped portion of Q_{HP} that penetrates through the plasma is

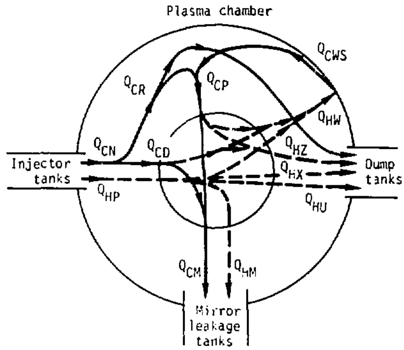

Fig. 3. Simplified flow diagram for the principal hot and cold particle flows.

shown entering the dump tanks as Q_{HU}. These hot neutrals are assumed to be converted to cold molecules on the walls of the dump tanks where they become direct contributions to Q_{1S} and Q_{2S}. Another portion of Q_{HP} charge exchanges with the plasma ions. Some of the hot neutrals produced, Q_{HX}, are assumed to enter each tank system where they are converted to cold gas molecules on the tank walls (only Q_{HX} into the dump tanks is shown in Fig. 3). The remainder of the hot charge-exchange neutrals produced by the hot injected neutrals is assumed to impinge on the plasma chamber walls.

The plasma chamber wall is assumed to convert all the impinging particles, Q_{HW}, to cold neutral molecules, which come off the wall as Q_{CWS}. (Some of the hot particles impinging on the plasma chamber wall may bury themselves in the wall material and/or cause sputtering of wall material. We neglect both of these effects in the present analysis.)

Finally, in this steady-state case, hot ions flow out the mirror exits at a rate Q_{HM}, which is equal to the portion of Q_{HP} that does not penetrate or charge exchange.

Once all the contributions to $Q_{1S}(K)$, $Q_{2S}(K)$ and Q_{CWS} are evaluated, the basic 2N + 1 Eqs. (1), (2), and (3) can be rewritten in a more convenient form for computer coding. The expressions for these source flow terms, as well as the steps in obtaining the final set of equations, are described in detail in Ref. 1.

Computer Program

The computer code simulates the physical model described in the preceding section of this paper. The basic Eqs. (1), (2), and (3) are coupled, linear algebraic equations, where the unknowns $P_1(K)$, $P_2(K)$, and P_{PC} correspond to the pressures in the N tank systems and the plasma chamber. The equations are solved simultaneously by the method of Householder reflections.[3] For a vacuum system where all N (nonidentical) peripheral tank systems have two chambers, 2N + 1 linear independent equations in 2N + 1 unknowns result. For a model where some peripheral tank systems consist of only one chamber, the tank K1 equations are no longer meaningful and are not included in the model. The tank K2 equations are the applicable equations for one chamber tank systems, and the input data for such tank systems must be entered for tank K2.

In the preceding discussion, the expression "non-identical" tank system refers to the fact that if identical tank systems, i.e., identical with respect to all input variables, were to be input as individual tank systems, dependent linear equations would result. Therefore, identical tank systems must not be input separately. The code has an input variable that is to be set equal to the number of identical tank systems, and the values for those tank systems are to be input only once. The code then manipulates the appropriate variables internally such that the identical tank systems are correctly modeled.

The input data consist of the following items: the number of cases to be run, the number of (non-identical) peripheral tank systems, the number of identical tank systems of each type, the number of chambers in each tank system, the input gas sources, the pumping speeds, the conductances, and the F values. The F values are a set of fractions specifying where the directed, non-random particles go. A complete list of the input variables and their definitions is found in Ref. 1.

To minimize the user's effort in the use of the code, there are default values for all of the input variables. The physical situation that the default F values were chosen to model corresponds to a central plasma chamber without a plasma. Thus, there is no ionization, charge exchange, magnetic confinement or magnetic leakage of particles in the plasma chamber, and the plasma chamber becomes no different than the other chambers. The default case assumes one-chamber peripheral tank systems with each tank system being unique. The default number of peripheral tank systems is four. All input gas sources, pumping speeds, and conductances have default values of zero. Therefore, to have a meaningful input data set, some of the input gas sources, pumping speeds, and conductances must be specified. Default values for all input variables are reassigned after the execution of each case. The default values for all of the input variables appear with their definitions in Ref. 1.

For conventional multi-chamber vacuum problems (no plasma), the GASBAL code can handle up to five chambers in series plus any number of two-chamber tank systems connected to the central chamber (ie., the former plasma chamber). The only trick required is to make the plasma "disappear". Our choice of default values on all of the hot particle flows automatically achieves this goal, so that the user can simply "ignore" the plasma. In addition, the equation in the code for the plasma chamber wall fluxes already includes a wall pumping speed for the cold background gas, S_{PCW}. For the case with no plasma, the plasma chamber wall equation becomes:

$$Q_{CWS} = -P_{PC}\, S_{PCW}.$$

Thus, the former cold gas source flow caused by wall reflux, Q_{CWS}, becomes a cold gas sink flow caused by pumping at the plasma chamber wall.

The code has a provision for treating different chamber temperatures. We assume that gas molecules instantaneously take the temperature of their respective chambers. The code performs all of its internal calculations at one temperature (T = 293 K), and then adjusts the results for the specified chamber temperatures. From the user's standpoint, this means that all input sources (both cold molecular gas and energetic atoms) must have the units of standard molecular Torr-ℓ/s, ie., 1 standard molecular Torr-ℓ/s = 3.29×10^{19} molecules/s = 6.58×10^{19} atoms/s = 5.19 molecular "amps" = 10.4 atomic "amps".

The pressures and number densities calculated and printed out for the specified chamber temperatures may be calculated for any other temperature by the following:

$$P(T_2) = P(T_1)\sqrt{\frac{T_2}{T_1}}\ , \text{ and}$$

$$n(T_2) = n(T_1)\sqrt{\frac{T_2}{T_1}}\ .$$

All the cold gas flow quantities that are printed out are correct for any chamber temperatures. This is because the decrease in density n with increasing chamber temperature is exactly offset by the increase in the average thermal speed.

The computer solution includes the following items: the cold gas pumped in each duct and chamber, the directed cold gas flow onto the plasma, the random cold gas flow onto the plasma, the pressure in each chamber, and the number density in each chamber.

Typical Mirror Machine Problem

We used GASBAL to analyze the proposed MX vacuum system. Of particular interest is the ratio of cold gas current impinging on the plasma to the injected neutral beam current. (Plasma buildup theory yields a maximum ratio above which plasma cannot be sustained.)

The MX vacuum system has been described earlier (Fig. 1). All of the peripheral tanks are to be lined with liquid-helium-cooled cryopanels. These cryopanels are protected by liquid-nitrogen-cooled chevron baffles. The resulting effective black hole area of the cryopanels is taken to be one-fifth of the actual surface area. All surfaces, except the cryopanels, are assumed to be at 77 K. All conductances are assumed to be orifices or ducts without internal cryopanels or other pumping.

Four basic cases involving changes only in the configurations of the beam dump tanks and mirror leakage tanks (or end tanks) were studied:

case 1: no beam dump tanks, mirror leakage tanks connected to the plasma chamber by a simple orifice of large conductance

case 2: with beam dump tanks, mirror leakage tanks as in case 1 case 3: no beam dump tanks, addition of a duct on the mirror leakage tanks, which lowers the conductance to the plasma chamber by two orders of magnitude

case 4: with beam dump tanks, mirror leakage tanks as in case 3

The key results for these four cases are plotted in Fig. 4. In the upper figure, the ratio of the total cold molecular gas current impinging on the plasma to the hot neutral atom current impinging on the plasma, I_{COP}/I_{HP}, is plotted as a function of the plasma radius. In the lower figure, the resulting steady-state cold background gas pressure in the plasma chamber, P_{PC}, is shown.

These cases are all for the conditions listed in the first column of Table 1 (a complete listing of the input for these calculations is given in Ref. 1). All calculations were done for deuterium gas with a leakage source flow of cold deuterium molecules of 35.5 Torr·ℓ/s (184 molecular "amps") from each of the two neutral beam sources. The corresponding hot neutral beam flow was 4.47 molecular Torr·ℓ/s of deuterium atoms (46.5 atomic "amps") from each injector source.

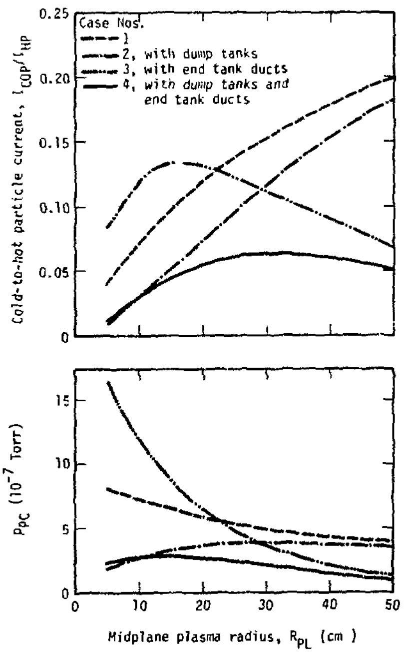

Fig. 4. Effect of configuration changes of the MX vacuum system on the ratio of cold-to-hot particle currents impinging on the plasma.

For these conditions the ratio of cold to hot particle currents entering the entire system is about 4.0. As can be seen from Fig. 4, the ratio of cold to hot particle currents impinging on the plasma is roughly two orders of magnitude less than this value, and depends on the plasma radius and the particular vacuum system configuration employed. The value of I_{COP}/I_{HP} that the plasma can tolerate in steady-state without being quenched must come from a separate plasma physics analysis; typical results of such analyses indicate that the value lies between 0.05 and 0.10.

For the simplest vacuum system configuration, case 1, Fig. 4 shows that the larger the plasma radius, the more cold gas impinges on it, even though the plasma chamber pressure decreases with radius. If beam dump tanks are added, the curve for case 2 shows that the cold gas impinging on the plasma is reduced for all plasma radii. However, because the neutral beam penetration fraction, F_{HUT}, decreases as the plasma gets larger, the fractional reduction in cold gas impinging on the plasma diminishes with increasing plasma radius.

We next consider case 4, where we retain the dump tanks and add low-conductance ducts to the mirror leakage tanks. Figure 4 shows a dramatic decrease in I_{COP}/I_{HP} at the larger plasma radii. This is due to the more effective pumping of the mirror leakage flows in the mirror tanks, which significantly reduces the cold gas pressure in the plasma chamber, P_{PC}, for the larger radii.

Finally, we consider case 3 where we eliminate the beam dump tanks and retain the small conductances to the mirror leakage tanks. Case 3 is significantly worse than case 4, as expected. Rather surprisingly, it is also worse than case 1 at the smaller plasma radii, because as the plasma radius decreases, the beam penetration fraction rises rapidly, causing the plasma chamber pressure to increase rapidly also, as shown on Fig. 4. At smaller plasma radii, P_{PC} for case 3 becomes larger than the pressure in the mirror leakage tanks. Consequently, the small conductance ducts to the mirror leakage tanks become detrimental. Removing them, as in case 1, allows the cold gas to flow from the plasma chamber into the mirror leakage tanks more easily, resulting in a much lower steady-state pressure in the plasma chamber.

The configuration of case 4 (with dump tanks and mirror leakage ducts) was selected for further investigation. (Figure 4 shows that for the nominal MX plasma radius of 20 cm, the configuration of case 2 without the mirror leakage ducts may also be adequate.)

Because many of the key F factors and other parameters can only be estimated, significant uncertainties exist in the input data. Additional calculations were made to test various assumptions, a few of which are described in the following paragraphs.

In case 4, none of the cold gas entering the plasma chamber was assumed to impinge directly on the plasma (i.e., $F_{CD} = Q_D = 0$), and 10% of the hot charge-exchange neutrals were assumed to enter the side tank, while the remaining 90% impinged on the plasma chamber wall. We investigated three variations of case 4. In case 4a, F_{CD} was varied as an increasing function of plasma radius to simulate the direct interception by the plasma of some of the random cold gas leaking in from the peripheral tanks. In case 4b, an additional 0.15% of the total cold gas from the neutral beam sources was assumed to free-stream directly onto the plasma. In case 4c, in addition to the above changes, 100% of the hot charge-exchange neutrals was assumed to impinge on the plasma chamber walls. None of these more pessimistic assumptions changed I_{COP}/I_{HP} very much. To be conservative, the most pessimistic case (4c) has been chosen as the reference design point for the nominal 20-cm radius plasma. The value of I_{COP}/I_{HP} for this case is 0.066. The data for this reference design point are summarized in the second column of Table 1.

The final series of calculations was essentially a sensitivity analysis of various important parameters for the reference design point. Some of the results are plotted in Fig. 5. In the top half of Fig. 5, four of the more important F factors were varied from the reference design values to ascertain the sensitivity of the cold gas flow on the plasma to uncertainties in these factors. As can be seen from the figure, if F_{HXT}, the hot neutral beam charge-exchange fraction, is significantly larger than our estimated reference value, the cold gas flow, I_{COP}, could become large enough to quench the plasma.

From the bottom half of Fig. 5, we see that a significant decrease in all the pumping speeds in

Table 1. *Key input parameters for MX example.*

Input parameters	Cases 1 – 4	Reference design point (case 4c)
Gas molecular weight (deuterium)	4.0	4.0
I_{COLD}/I_{HOT} entering system	3.96	3.96
Plasma radius, R_{PL} (cm)	variable	20.0
Direct cold gas fraction on plasma, F_{CD}	0	0.0156
Beam penetration fraction, F_{HOT}	increasing function of R_{PL}	0.262
Beam charge-exchange fraction, F_{HXT}	increasing, then decreasing function of R_{PL}	0.194
Cold gas charge exchange fraction, F_{CX}	0.57	0.57
Fraction of charge exchange neutrals that impinge on the plasma chamber walls, $F_{H\ TO\ WALL}$	0.9	1.0
Plasma pumping speed, S_{PL} (ℓ/s)	Increasing function of R_{PL}	1.87×10^6
	Values for case 4 and 4c	
$S_1(1)$, $S_1(2)$, (ℓ/s at 293 K)	8.78×10^5	
$S_2(1)$,	5.18×10^5	
$S_2(2)$,	6.90×10^5	
$S_2(3)$, $S_2(4)$,	3.12×10^6	
$C_{11}(1) = C_{12}(1)$, (ℓ/s at 293 K)	1.32×10^4	
$C_{11}(2) = C_{12}(2)$,	1.46×10^5	
$C_{22}(1) = C_{2P}(1)$,	6.50×10^4	
$C_{22}(2) = C_{2P}(2)$,	1.06×10^5	
$C_{22}(3) = C_{2P}(3)$,	3.12×10^4	
$C_{22}(4) = C_{2P}(4)$,	4.28×10^6	

all the tanks, due, for example, to an overestimate of the effective black hole areas of the chevron-protected cryopanels, could also result in plasma quenching. Additional calculations demonstrated that the cold gas flow, I_{COP}, is most sensitive to changes in the pumping speed in the side tank, $S_1(4)$ (see Table 1 and Fig. 2). Individual changes in the other pumping speeds are relatively ineffective in changing I_{COP}.

Finally, each conductance was varied individually. We found that only changes in the conductance to the side tank, $C_{22}(4)$, affect I_{COP} significantly. It is interesting to note that increasing this conductance rather than decreasing it, reduces I_{COP}/I_{HP}. This is because, for our cases, the pressure in the side tank is always lower than the plasma chamber pressure, so that increasing the conductance between the two chambers results in a decrease in P_{PC} and hence a decrease in I_{COP}/I_{HP}.

These kinds of calculations provide very useful information to vacuum system designers, particularly for complex systems such as those required for fusion machines.

REFERENCES

1. M. A. Hoffman, T. R. Roose and G. A. Carlson, "The GASBAL Code: Equations and Solution Method for Calculating Steady-State Conditions in Multi-Chamber Vacuum Systems for Fusion Machines," Lawrence Livermore Laboratory report in preparation.

2. R. E. Vonholdt, "MLR," Lawrence Livermore Laboratory, CIC Rept. F3-001, 1969.

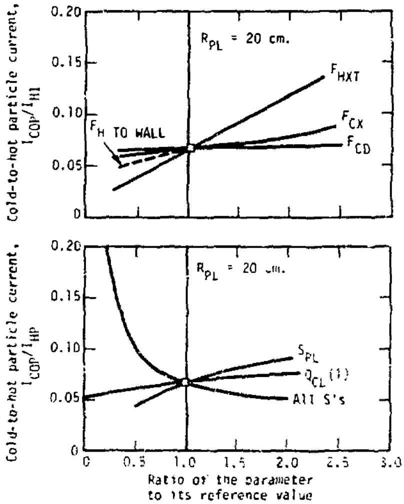

Fig. 5. Sensitivity of the ratio of cold-to-hot particle currents impinging on the plasma to variations in some of the MX vacuum system and plasma parameters.